Video Article

Ischemic Tissue Injury in the Dorsal Skinfold Chamber of the Mouse: A Skin Flap Model to Investigate Acute Persistent Ischemia

Yves Harder[1], Daniel Schmauss[1], Reto Wettstein[2], José T. Egaña[1], Fabian Weiss[1], Andrea Weinzierl[1], Anna Schuldt[1], Hans-Günther Machens[1], Michael D. Menger[3], Farid Rezaeian[4]

[1]Department of Plastic Surgery and Hand Surgery, Klinikum rechts der Isar, Technische Universität München

[2]Department of Plastic, Reconstructive, Aesthetic and Hand Surgery, University Hospital of Basel

[3]Institute for Clinical and Experimental Surgery, University of Saarland

[4]Division of Plastic and Hand Surgery, University Hospital Zurich

Correspondence to: Yves Harder at yves.harder@yahoo.com

URL: https://www.jove.com/video/51900
DOI: doi:10.3791/51900

Keywords: Medicine, Issue 93, flap, ischemia, microcirculation, angiogenesis, skin, necrosis, inflammation, apoptosis, preconditioning, persistent ischemia, *in vivo* model, muscle.

Date Published: 11/17/2014

Citation: Harder, Y., Schmauss, D., Wettstein, R., Egaña, J.T., Weiss, F., Weinzierl, A., Schuldt, A., Machens, H.G., Menger, M.D., Rezaeian, F. Ischemic Tissue Injury in the Dorsal Skinfold Chamber of the Mouse: A Skin Flap Model to Investigate Acute Persistent Ischemia. *J. Vis. Exp.* (93), e51900, doi:10.3791/51900 (2014).

Abstract

Despite profound expertise and advanced surgical techniques, ischemia-induced complications ranging from wound breakdown to extensive tissue necrosis are still occurring, particularly in reconstructive flap surgery. Multiple experimental flap models have been developed to analyze underlying causes and mechanisms and to investigate treatment strategies to prevent ischemic complications. The limiting factor of most models is the lacking possibility to directly and repetitively visualize microvascular architecture and hemodynamics. The goal of the protocol was to present a well-established mouse model affiliating these before mentioned lacking elements. Harder *et al.* have developed a model of a musculocutaneous flap with a random perfusion pattern that undergoes acute persistent ischemia and results in ~50% necrosis after 10 days if kept untreated. With the aid of intravital epi-fluorescence microscopy, this chamber model allows repetitive visualization of morphology and hemodynamics in different regions of interest over time. Associated processes such as apoptosis, inflammation, microvascular leakage and angiogenesis can be investigated and correlated to immunohistochemical and molecular protein assays. To date, the model has proven feasibility and reproducibility in several published experimental studies investigating the effect of pre-, peri- and postconditioning of ischemically challenged tissue.

Video Link

The video component of this article can be found at https://www.jove.com/video/51900/

Introduction

Coverage of exposed tendon, bone and implant material in reconstructive surgery relies on the use of flaps. A flap is a block of tissue that is transferred on its vascular pedicle that guarantees arterial inflow and venous outflow. Despite broad expertise and the availability of a variety of flaps to be transferred, ischemia-induced complications ranging from wound breakdown to total tissue loss are still encountered. Whereas conservative treatment and healing by secondary intention can be expected after minor tissue necrosis, significant flap necrosis usually requires surgical revision, including debridement, wound conditioning and secondary reconstruction. This increases morbidity, prolongs hospital stay and consequently leads to increased health care costs.

Flaps with an undefined pattern of vasculature or randomly perfused areas in the distal zone most remote from the arterial inflow are particularly prone to ischemic damage. Accordingly, numerous experimental and clinical studies have evaluated the development of necrosis in both, axial pattern flaps (defined blood supply) and random pattern flaps (undefined blood supply)[1-3]. The main findings are commonly based on macroscopic evaluation of the size of the necrotic area. In order to assess the causes and mechanisms of tissue necrosis more in detail, several studies focused on the analysis of microcirculation. Different techniques have been used to measure tissue perfusion, including the analysis of tissue oxygen tension using polarographic electrodes[4-5], as well as the measurement of blood flow using laser Doppler flowmetry[6-7], dye diffusion[8], and microspheres[9-10]. These techniques, however, only allow for measuring indirect parameters of tissue perfusion and do not enable any morphological analysis of the microhemodynamic processes within an individual area of interest of a flap.

Sandison is known to be the first who has used a transparent chamber for prolonged *in vivo* studies, which he performed in rabbits[11]. In 1943 — approximately 20 years later — Algire was the first to adapt such a transparent chamber to be applicable in mice in order to study the behavior of micro-implants of tumor cells[12]. Due to the fact that mice are so-called loose skin animals and after some technical refinements over the following years, Lehr and co-workers were able to adapt such a dorsal skinfold chamber developing a smaller and lighter titanium chamber. This chamber enabled evaluation using intravital fluorescence microscopy, a technique that allows direct and repetitive visualization of a number of

morphologic and microcirculatory features and their changes over time under different physiological and pathophysiological conditions, such as ischemia-reperfusion injury[13].

In the investigation of perfusion of skin, muscle and bone flaps under normal and pathological conditions two trends occurred: First, the “acute” flap models that do not use the dorsal skinfold chamber such as the pedicled ear flap in the mouse[14], the laterally based island skin flap in the hamster[15] and the pedicled composite flap in the rat[16]. Second, the “chronic” flap model where the combination of a flap with a dorsal skinfold chamber permits repetitive microcirculatory analyses over several days with intravital fluorescence microscopy. It consists of a randomly perfused musculocutaneous flap that is integrated in the skinfold chamber of the mouse [17]. Its width-to-length ratio was chosen that a situation of acute persistent ischemia consistently results in ~50% flap tissue necrosis 10 to 14 days after flap elevation. This reproducible extent of tissue necrosis allows further evaluation of both, protective (*i.e.*, development of less necrosis) and detrimental factors (*i.e.,* development of more necrosis) on flap pathophysiology. During the last years, several experimental publications demonstrating the effect of different pre-, peri- and post-conditioning procedures, including the administration of tissue-protective substances[18-24] and the local application of physiologic stressors such as heat[25] and shockwaves[26], have emerged.

The quantitative analyses of necrosis, microvascular morphology and microcirculatory parameters can further be correlated to immunohistochemical analyses and protein assays. Different proteins and molecules including vascular endothelial growth factor (VEGF), nitric oxide synthases (NOS), nuclear factor kappa B (NF-κB) and heat shock proteins (HSP-32: heme-oxygenase 1 (HO-1) and HSP-70) have been shown to play a role in tissue protection. Based on this chamber flap model, two modifications have been developed in order to analyze neovascularization and microcirculation during skin graft healing[27] and angiogenic developments in a pedicled flap with axial pattern perfusion[28]. We present a reproducible and reliable model that includes an ischemically challenged musculocutaneous flap in the mouse skinfold chamber. This model allows visualization and quantification of the microcirculation and hemodynamics by intravital epi-fluorescence microscopy.

Protocol

NOTE: Prior to implementation of the presented model, the corresponding animal protection laws must be consulted and permission must be obtained from the local authorities. In this work, all experiments were performed in conformity with the guiding principles for research involving animals and the German legislation on protection of animals. The experiments were approved by the local animal care committee.

1. Animal Preparation and Surgical Elevation of the Flap

1. Keep animals in single cages at room temperature of 22–24 °C and at a relative humidity of 60–65% with a 12-hr day-and-night cycle. Allow mice free access to drinking water and standard laboratory chow. Always maintain sterile conditions during survival surgery.
2. Anesthetize the mouse by intraperitoneal (i.p.) injection of 0.1 ml saline solution per 10 g bw containing 90 mg/kg bw ketamine hydrochloride and 25 mg/kg bw dihydroxylidinothiazine hydrochloride. Anesthesia is necessary for animal preparation, surgery and subsequent microscopy. Confirm proper anesthetization by checking the response to a painful stimulus. During the time of anesthesia, apply vet ointment on eyes to prevent dryness.
3. After induction of sufficient anesthesia, depilate the back with an electric shaver. Hereafter, apply depilation cream to the shaved area to remove the remaining hair.
4. During residence time of the depilation cream of ~7–10 min, prepare instruments, including skin forceps and micro forceps, scissors and micro scissors, suture material and a marker pen. Disinfect and prepare the titanium chamber by applying the two screws with the nut at the chamber’s base and by fixing self-adhesive foam (**Fig. 1 A-C**) around the window of the chamber’s counterpart to guarantee tightness of the chamber system.
5. Remove all depilation cream from the back by washing it off with tepid water. Then dry and disinfect the skin with an alcohol-containing solution.
6. Place the mouse in prone position and define the midline of the back. Grasp the skin centrally and lift it up to create a fold (**Fig. 2A**). By trans-illumination using any kind of light source, decide where to provisorily place the titanium frame (**Fig. 2B**). Make sure that the distal branches of the lateral thoracic artery (LTA) cranially and the deep circumflex iliac artery (DCIA) caudally course through the center of the chamber’s window (**Fig. 2B-D**). Once the positioning of the chamber is done, perforate both layers of the skin at the very bottom of the fold for later fixation of the titanium frame. Now remove the titanium frame, place the mouse in prone position and redefine the midline of the back if necessary.
7. Outline the flap perpendicular to the spine starting at the midline with a width-to-length ratio of 15 x 11 mm to result in a laterally based and randomly perfused flap. Then outline an additional skin area of 2 mm extending to the contralateral side (**Fig. 2C, D**). This area is picked with the forceps and later sutured to the titanium frame without interfering with the visible flap area.
8. Following final marking, incise the flap. In doing so, transect both the LTA and DCIA and elevate the flap (**Fig. 2E**). There is no need for coagulation or ligation of the transected vessels.
9. Place the chamber’s screw through the previously made skin perforations (**Fig. 2F**) and fixate the skinfold both anteriorly and posteriorly within the chamber’s frame of the elevated flap to the backside part of the frame using the holes of the chamber’s frame and a 5-0 interrupted sutures (**Fig. 2G**).
10. Suture the vertical limbs of the flap back to the surrounding skin by means of 5-0 interrupted sutures (**Fig. 2H, I**).
11. Excise a hemi-circular area of skin lateral to the small skin strip of 2 mm, *i.e.*, on the other side of the flap to observe the flap’s vasculature. This allows direct view through the observation window of the chamber that has a surface of 90 mm^2.
12. Remove the gelatin-like loose areolar tissue from the striated muscle using microsurgical instruments and optical magnifying lens or microscope in order to improve the image quality during microscopy. Try not to damage vessels within the muscular tissue layers.
13. Finally, seal the chamber by mounting the counterpart of the frame that has previously been endued with self-adhering strips of foam anteriorly, cranially and posteriorly, bedew the flap with topical bisbenzimide and saline (**Fig. 2J**). Thereafter, apply the observation window with a cover glass using a snap ring. Try not to entrap any air blisters under the glass (**Fig. 2K, L**). The skin will adhere to the cover glass by adhesion forces.

2. Intravital Epifluorescence Microscopy

1. Wait 24 hr after surgical preparation for the first microscopic analysis for ideal optical quality. This analysis represents the baseline of microscopy and is repeated at day 3, 5, 7 and 10 after surgery. Each time, anesthetize the mouse as described in step 1.2. Place the animal in a lateral decubital position on a custom-made Plexiglas carrier. That way, the muscular tissue layers of the flap adhering to the cover glass are facing up-wards.
2. Inject 0.05 ml of 5% green fluorescence dextran (molecular weight 150,000) and 0.05 ml 1% highly fluorescent Rhodamine family dye in a tail vein or the retro-bulbar venous plexus. The green fluorescent dextran stains the non-cellular components of the blood if applied intravenously (i.v.). The fluorescent Rhodamine stains leukocytes and platelets that can be distinguished from other cellular and non-cellular components. Finally, bisbenzimide stains nuclear components that emit more or less fluorescence according to the state of condensation.
3. Subsequently, place the mouse under the microscope. Ensure the microscope includes a LED system — LED beam combinations for 470 & 425 nm, 365 & 490 nm, and 540 & 580 nm as well as the corresponding filter sets (62 HE BFP/GFP/HcRed, range 1: 350–390 nm excitation wavelength, split 395 nm / 402–448 nm; range 2: 460–488 nm, split 495 nm / 500–557 nm; range 3: 567–602 nm, split 610 nm / 615 nm to infinite. 20 Rhodamine, range: 540–552 nm, split 560 nm, emission 575–640 nm).
4. Record the stills and motion-pictures using a charge-coupled device video camera and save them on a computer hard disk for further off-line analysis.
5. Use different objectives (2.5X, NA (numerical aperture) = 0.06 for panorama views of the chamber; 5X, NA = 0.16; 10X, NA = 0.32; 20X, NA = 0.50; 50X, NA = 0.55) for recordings of the regions of interest.
6. Virtually, divide the flap surface that is visible through the chamber's window into three areas of equal height, *i.e.*, a proximal, a central, and a distal area most remote from the vascular inflow (**Fig. 3F**). For image acquisition, proceed the following way at each observation time point:
    1. Scan the tissue image by image within the chamber's window from proximal to distal using the 5X objective.
    2. In each area of the flap, select second- or third-order arterioles and their accompanying venules with easily identifiable branching patterns. Using the 5X, 10X, or 20X objective, make printouts of the arteriolovenular bundles in order to easily re-localize the bundles throughout the whole observation period.
    3. With the 20X objective and the 50X objective, further record 5–6 capillary fields and "apoptotic" fields per area of the flap respectively. All images recorded with the 10X and 20X objectives use the blue light (fluorescent dextran) and green light (Rhodamine) filter, whereas images recorded with the 5X and 50X objective use blue light (fluorescent dextran) and white light (Bisbenzimide) filter, respectively.

3. Analysis of Recorded Data

NOTE: With the use of a computer-assisted image analysis system quantify all recorded parameters off-line as follows[29].

1. Measurement of the area of non-perfused, respectively necrotic tissue (mm^2).
    1. Use the complete scanned chamber window image recorded with the 5X objective (from 2.6.1) and the fluorescent dextran to measure non-perfused respectively necrotic tissue. Use "AreaBo" function to measure the non-perfused dark area: Border the non-perfused area and calculate the area in mm^2 by using the software's Area measurement algorithms.

2. Measurement of microvascular diameter in arterioles, capillaries and venules (µm).
    1. Load video or pictures from the recorded AV-bundles or the capillary fields into the software. For best results use the stills or videos with the highest magnification where definite borders of the vessel are clearly visible.
    2. Use the "DiamPe" function of the software to make sure the measurements are performed perpendicular to the vessel's wall. To do so mark two points on the vessel's wall and with the third click mark the perpendicular diameter of the vessel. The software will perform the measurement in µm.
    3. Repeat the measurements on the same vessels for all recordings at the same place. Measure multiple capillaries to accumulate average diameter.

3. Analysis of red blood cell (RBC) velocity in arterioles, capillaries and venules (mm/sec).
    1. For arteriolar red blood cell (RBC) velocity (mm/s) measurements use the "VeloLSD" function of the software and choose the same vessels in the fluorescent dextran window for which the diameters have been measured.
    2. Analyze it with the computer-assisted image analysis system using the line shift method, which is on the basis of the measurement of the shift (mm) of an individual intravascular gray level pattern over time (sec).

4. Measurement of volumetric blood flow in vessels (pl/sec).
    1. Calculate volumetric blood flow (pl/sec) in arterioles, venules and capillaries from RBC velocity and vessel cross-sectional area ($\pi * r^2$) according to the equation of Gross and Aroesty, that is, $Q = V * \pi * r^2$, assuming a cylindrical vessel shape[30].

5. Measurement of functional capillary density of RBC-perfused capillaries (nutritive perfusion: cm/cm^2).
    1. Load a recorded fluorescent capillary field with 20X objective magnification into the software. Use the "DensLA" function to measure functional capillary density of RBC-perfused microvessels.
    2. Trace the perfused capillaries with the cursor and mark the perfused vessels. Do not mark non-perfused capillaries, arterioles or venules. The software will measure functional capillary density of the perfused capillaries in cm/cm^2. Repeat the steps for the other recorded capillary fields.

6. Measurement of tortuosity of the microvessels (microvascular remodeling), early signs of angiogenesis such as bud and sprout-formation and newly formed microvessels.

1. Load recorded videos or frames of fluorescent capillary fields into the software. Identify gyrose vessels and use the "TorqIx" function of the software. Trace the definite vessel flow with the course and end with a right click. The software will draw a straight line for the direct way and will set it in relation with the traced path.
   NOTE: Watch out for signs of angiogenesis such as buds, sprouts and newly formed capillaries, which usually emanate perpendicularly from the pre-existing capillaries. Measure the density of these newly formed vessels as described in step 3.5.

7. Identification of characteristics for apoptotic cell death, such as nuclear condensation, fragmentation and/or margination (cells/mm^2).
   1. Load Bisbenzimide-recorded videos (50X objective) into the software. Use the "DenseNA" function. Mark apoptotic cells according to the mentioned characteristics such as nuclear condensation, fragmentation and margination with a left click.
   2. After marking all characteristic cells throughout the video, click "N/A" in the software, which will automatically count all marked cells and divide it throughout the area. The result will be apoptotic cells/mm^2.

8. Analysis of leukocyte adherence to the vascular endothelium representing inflammation. Intermittent adherence of leukocytes (rolling leukocytes; adherence < 30 sec: number of rollers/mm^2 endothelial surface) and firm adherence of leukocytes (sticking leukocytes; adherence > 30 sec: number of stickers/mm^2 endothelial surface).
   1. Analyze the inflammatory response by counting the number of Rhodamine labeled leukocytes that adhered to the endothelial lining of post-capillary venules for a time period of ≥30 sec ("stickers") and the intermittently adhering leukocytes (<30 sec, "rollers"). Venular leukocyte adherence is expressed as cells per mm^2 endothelial surface.

9. Measurement of intravascular and interstitial grey levels as a parameter for microvascular leakage (macromolecular extravasation E=E1/E2).
   1. Assess macromolecular leakage as a parameter of microvascular permeability after an i.v. injection of a fluorescent dextran. Densitometrically determine multiple grey levels in the tissue directly adjacent to the capillary vessel wall (E1), as well as in the marginal cell-free plasma of the vessel (E2). Then calculate macromolecular extravasation (E) as the ratio of E1/E2 [31].

4. Postoperative Care

1. Return the animal in a separate cage to avoid the company of other animals until fully recovered. Do not leave an animal unattended until it has regained sufficient consciousness to maintain sternal recumbency. Monitor animals daily for bleeding, local and systemic signs of infection and the position of the chamber.
2. Evaluate the general state of the animal by observing motor activity, body weight, signs of pain, tolerance to the dressing and auto-mutilation.
3. Keep the mice one per cage to avoid mutual manipulation of the chamber. At any sign of pain, apply Buprenorphine at a dose of 0.05–0.1 mg/kg bw, subcutaneously in 8 hr intervals.

5. Euthanasia and Explantation of the Skinfold Chamber

1. At day 10, sacrifice animals using an overdose of an anesthetic drug (150 mg/kg Pentobarbital).
2. Remove the chamber and sample the flap tissue for immunohistochemical and molecular protein assays. Sample tissues for conventional histology (formalin) and quantifiable protein assays (liquid nitrogen or dry ice).

Representative Results

Necrosis

The main endpoint of this model — tissue necrosis following flap elevation (*i.e.,* induction of acute persistent ischemia) — is repeatedly measured and illustrated macroscopically as shown in **Figure 3** over a period of 10 days. Final demarcation of flap necrosis usually occurs between day 5 and 7 after surgery and is characterized by a red fringe, *i.e.*, zone of vasodilation and microvascular remodeling, developing between the proximal vital and the distal necrotic zone of the flap (**Fig. 3D-F**). Untreated control mice usually develop a necrotic area of about 50% after 10 days that can be divided into three distinct areas: the well perfused proximal, the intercalated and critically perfused central area and the necrotic distal area (**Fig. 3F**). Previous studies of our group, as mentioned in the introduction, have shown protective effects after different preconditioning procedures, which are characterized by a shift of the critically perfused area from the central zone towards the distal zone of the flap.

Vessel parameters

Microvascular diameters and red blood cell (RBC)-velocity of arterioles and venules of various diameters as well as of neighboring capillaries are measured and the resulting volumetric blood flow is calculated off-line. This allows correlating both morphological and functional changes of distinct microvessels from day 1 to day 10 (**Fig. 4A-B**). In addition, the functional density of the RBC-perfused capillaries, the parameter for nutritive perfusion of the tissue, is analyzed. The capillaries are usually oriented in-parallel and present with diameters between 3-5 µm under physiologic conditions (**Fig. 4C**). Blood flow, functional capillary density and eventually oxygen tension of the tissue gradually decrease from proximal to distal to reach a threshold "of viability" (**Fig. 4C-E**), where the capillaries are not perfused anymore (**Fig. 4E**).

Microvascular remodeling and angiogenesis

Remodeling with dilation and increased tortuosity of the microvessels can be observed in all experimental groups undergoing flap preparation (*i.e.*, induction of acute persistent ischemia: **Fig. 4F**). However, in this model, the ischemic stimulus alone is not enough to induce angiogenesis as for example seen in a variety of preconditioning experiments with the hormone erythropoietin (**Fig. 4G-H**). The new functional microvascular

networks that usually develop from microvascular buds and sprouts emanating perpendicularly from the pre-existing in-parallel arranged capillaries are first visible between day 3 and 5.

Inflammatory response (leukocyte-endothelial interaction and apoptosis)

Acute persistent ischemia usually induces a considerable inflammatory response in untreated animals that is represented by adhering leukocytes to the microvascular endothelium. This inflammatory response is characterized by rolling (*i.e.*, intermittent adhesion of leukocytes to the vascular endothelium) and sticking (*i.e.*, firm adhesion of leukocytes to the vascular endothelium) leukocytes (**Fig. 5A-B**). In addition, an ischemia induced increase of apoptotic cells can be seen in all control animals with the characteristic signs of nuclear condensation, fragmentation and margination (**Fig. 5C-D**). Both, leukocyte-endothelial interaction and apoptosis are signs for the ischemia-induced inflammatory response and gradually increase with progressive microvascular dysfunction and decreased oxygen tension of the tissue (*i.e.*, along the “ischemic” axis of the flap proximal to distal (**Fig. 5A-D**)).

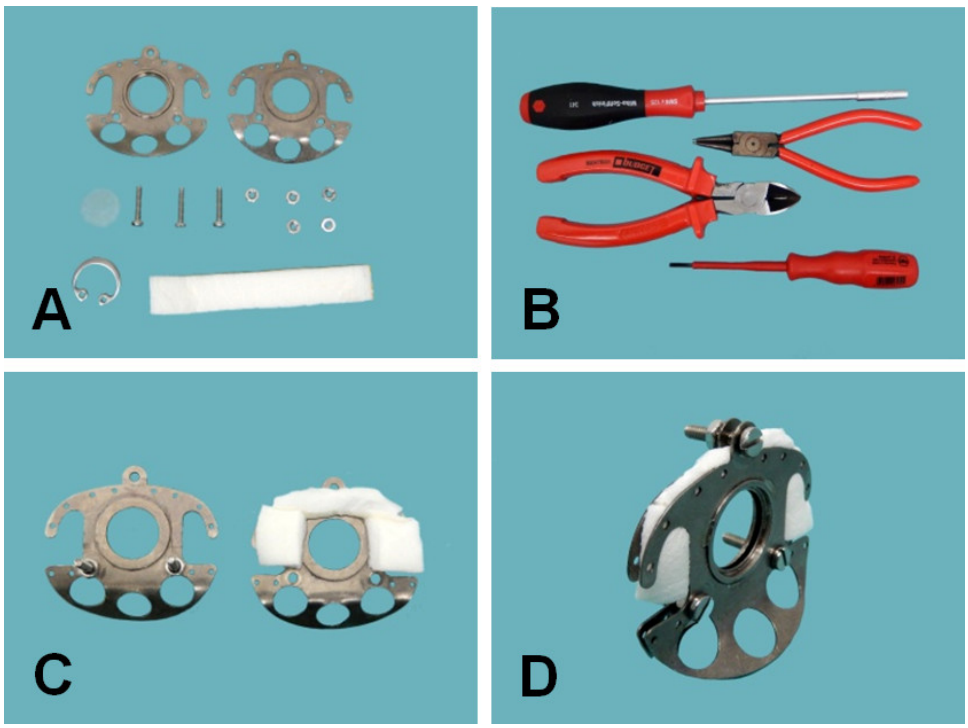

Figure 1. Illustration of the titanium chamber frame and all of its work pieces. (**A**) Disassembled frame consisting of two frame parts, three screws, five nuts, one piece of foam, a cover glass and a snap ring. (**B**) Required tools to assemble the frame including a hex nut driver, a snap ring plier and a wire cutter. A screwdriver is not required but recommended if chambers will be used several times. (**C**) Assembled single chamber parts. Left: Back side of the frame with two screws and attached nuts on the lower two holes. The back side is used to suture the frame onto the skin and bears the flap. Right: Assembled front side of the frame with attached foam to guarantee tightness. Note that all three screw-holes are kept free of foam. Make sure that none of the foam will be pressed into the observation window, which bears the cover glass. (**D**) Schematic assembled chamber frame without dorsal skinfold.

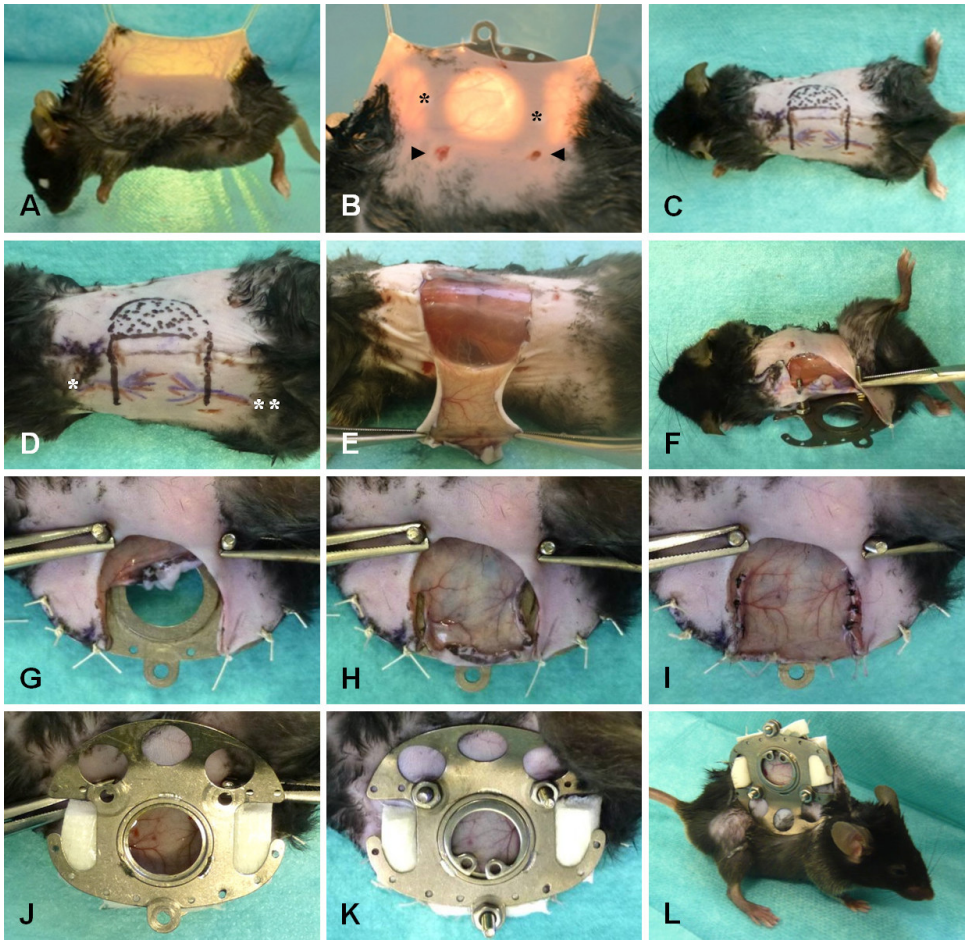

Figure 2. Illustration of the operative flap procedure and its implementation in the titanium dorsal skinfold chamber of the mouse. (**A**) Elevated trans-illuminated doubled dorsal skinfold of the mouse to visualize vascular architecture for outlining the position of the dorsal skinfold chamber. (**B**) The backside of the chamber's titanium frame has been positioned and aligned with the vessels. The incision of two holes for screws to attach the front side of the frame has been made. (**C** and **D**) Outlining of the flap on the dorsal skin laterally: The width-to-length ratio is 15 mm to 11 mm while centralizing the two perpendicularly arising vessels. A 2 mm distance to the contralateral side (unmarked area between thin flap outline and thick border) will be used to grasp the skin with forceps to elevate the flap. For the observation of the backside skin through the chamber window, additional tissue has to be removed (hatched area). (**E**) Elevated laterally based skin flap, demonstrating the randomly arranged vascular architecture originating from the base of the flap. The hatched area has been cut out, but is still attached to the flap and is removed in the next step (hanging skin below the forceps). (**F**) Mounting the back side of the chamber frame. The skin surface of the flap is on the backside and the “raw” surface under the glass window side. The chamber`s screws are stuck through the incised holes on both sides of the dorsal skinfold. (**G**) The surrounding skin, anteriorly and posteriorly, of the flap is fixed in the holes of the upper chamber rim. (**H**) The skin flap is stretched out and also sutured to the back side of the frame. To avoid dehydration of the flap, 0.9% sodium chloride solution is dripped onto the flap repeatedly. (**I**) The flap and the surrounding skin is completely fixed in the holes of the upper chamber rim. The flap is sutured back laterally into the adjacent dorsal skin to guarantee tightness of the chamber. (**J**) Mounting the foam-bearing counterpart of the frame, surrounding the observation window. (**K**) Completely mounted chamber: A cover glass is attached to the observation windows and sealed with a snap ring. A third screw is attached to the top of the frame for additional tightness. The window in the chamber allows repeated analyses of the microvasculature of the flap by intravital microscopy. For easier access during microscopy the three screws are shortened. (**L**) Awake and moving mouse with mounted dorsal skinfold chamber.

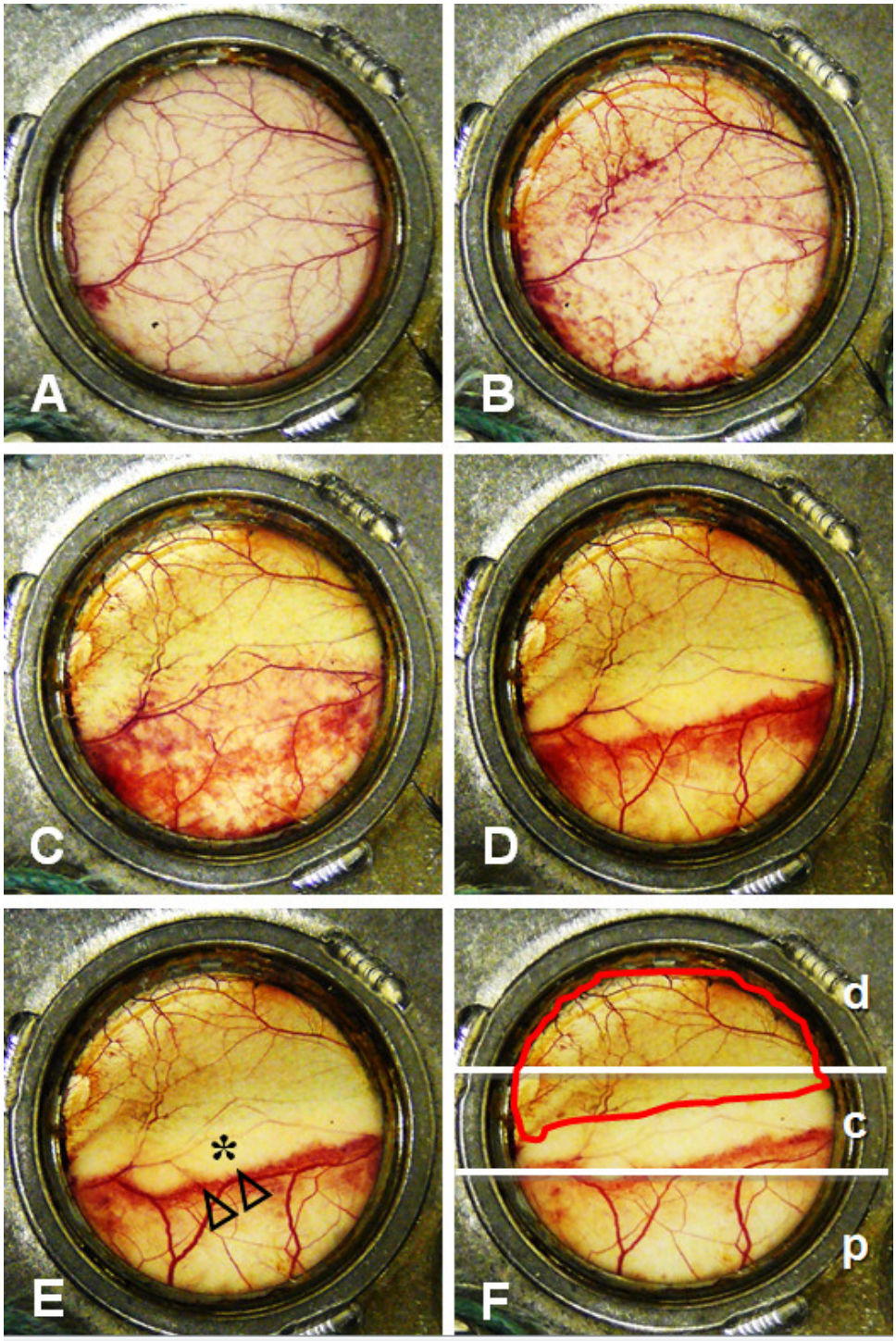

Figure 3. Presentation of the morphological development and demarcation of the flap necrosis at days 0 (immediately after flap preparation, A), 1 (B), 3 (C), 5 (D), 7 (E) and 10 (F). Final necrotic demarcation takes place between days 5 and 7 (D and E). Controls show a distinct zone of demarcation within the central flap area, including a red fringe and a white falx (double arrowhead and asterisk in E), reflecting a hyperemic response and microvascular remodeling as well as a non-perfused but potentially viable area delineating tissue necrosis developing distally (E). In panel F, the flap tissue is divided in three distinct areas by 2 horizontal lines: the well perfused proximal zone (at the base of the image), the critically perfused central zone (including the red fringe an the white "falx lunatica" corresponding to the penumbra in ischemic brain tissue after stroke injury) and the necrotic distal zone (circumferentially marked by red border). Magnification 16X.

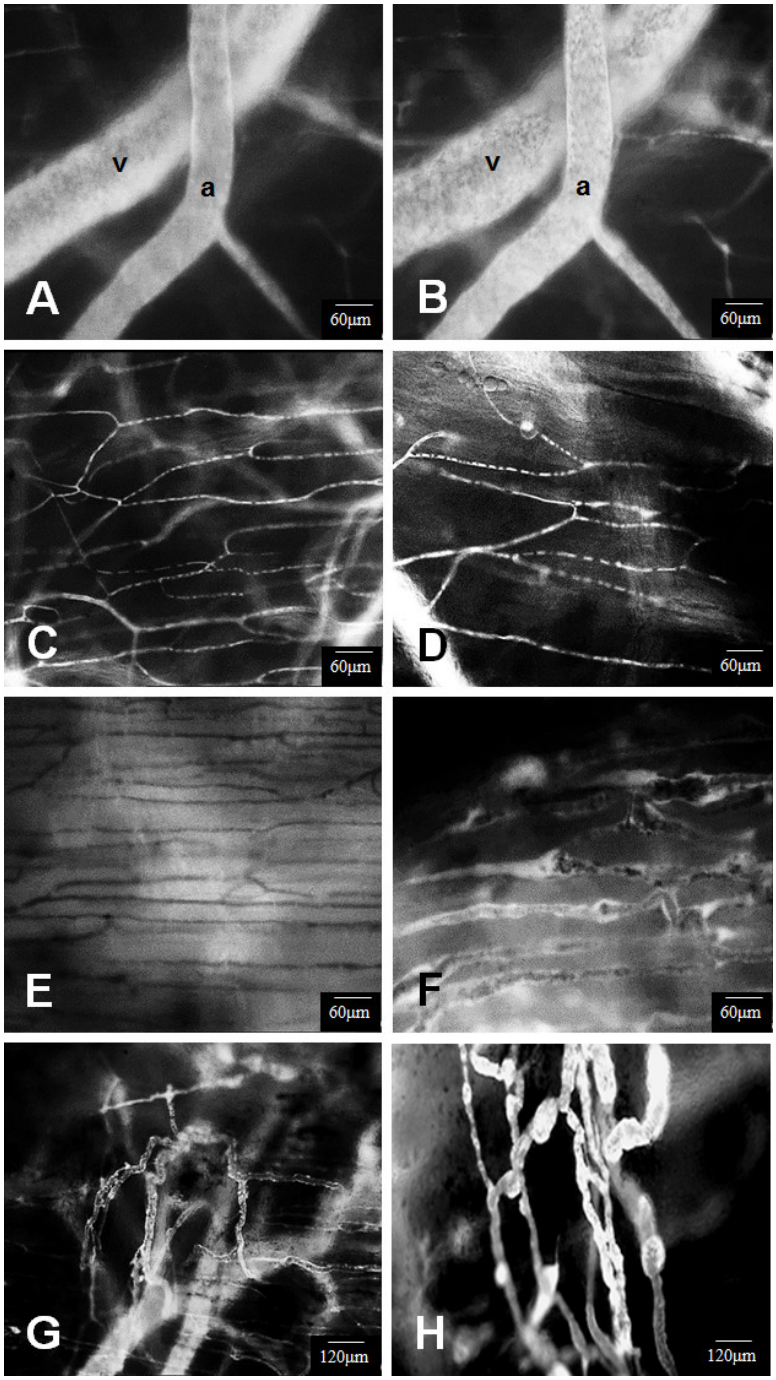

Figure 4. Intravital epi-fluorescence microscopy displaying images of arteriovenular (AV) bundles (A, B), capillary fields (C, D, E) and morphological changes such as remodeling (F) and angiogenesis (G, H). Intravital microscopy showing the same AV-bundle in a control animal (A, B) at day 1 (A) and 10 (B). Note the absence of dilatory response in controls over the whole observation period in both arteriolar (a) and venular (v) diameter. Images C, D and E demonstrate parallelly arranged capillaries in the well perfused proximal zone (C), critically perfused central transition zone (D) and the non-perfused necrotic distal zone (E) of the ischemic flap tissue. In the critically perfused central zone control mice only show vascular remodeling (F), characterized by in parallel arranged capillaries with dilation and increased tortuosity. In contrast, mice receiving erythropoietin before flap elevation as a preconditioning regimen show newly formed and perpendicularly arising capillaries, which are clearly distinguishable from normal pre-existing capillaries (G, H). This angiogenic response has not been observed in controls. Contrast enhancement with fluorescent dextran 150,000. Magnification 80X.

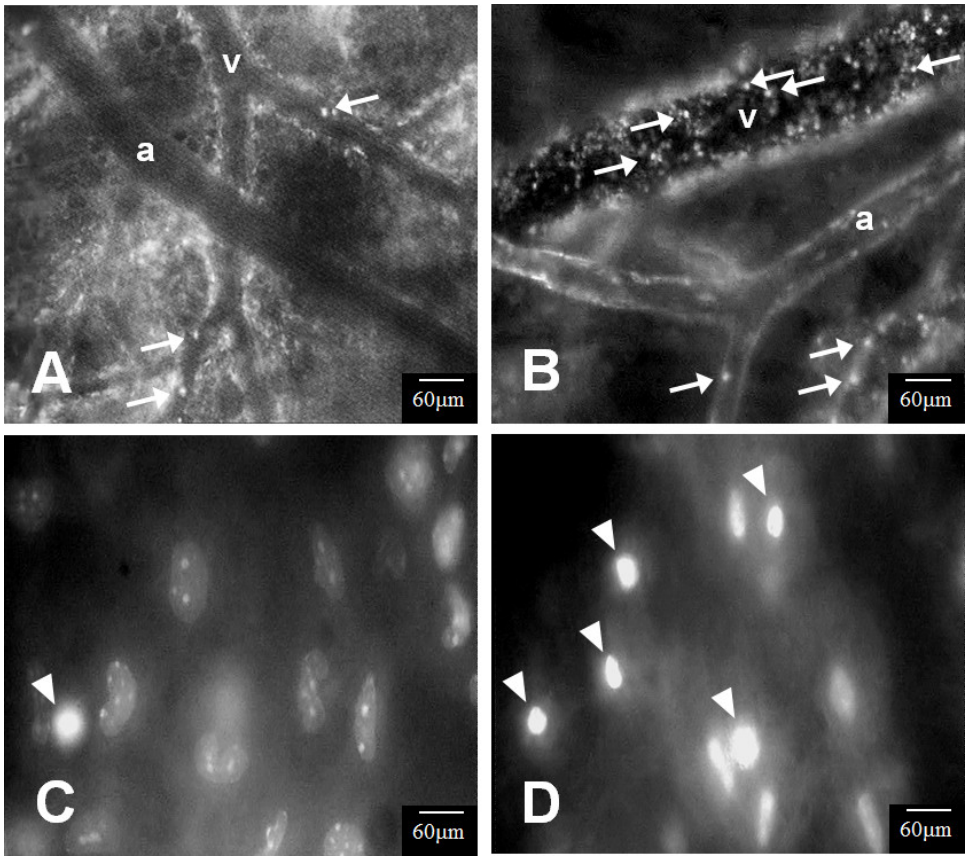

Figure 5. Intravital epi-fluorescence microscopy displaying AV-bundles in the well perfused proximal flap zone (A) and the critically perfused ischemic central transition zone of the tissue (B). Note the increased presence of adhering leukocytes (arrows) in postcapillary venules (v) and arterioles (a) within the ischemic flap zone (B) when compared the healthy proximal zone (A). Contrast enhancement with Rhodamine. Magnification 80X. Intravital epi-fluorescence microscopy displaying nuclear condensation indicating apoptotic cell death within the proximal (C) and critically perfused central flap area (D) of controls. An increased number of apoptotic cells (white arrows) is observed within the more ischemic central transition zone (D) when compared to the proximal zone (C). Contrast enhancement with Bisbenzimide. Magnification 250X.

Discussion

In order to decrease ischemic complications and thereby improve the clinical outcome, more detailed knowledge of pathophysiologic processes in critically perfused flap tissue is required. The development of new animal models that mimic acute persistent ischemia is therefore mandatory. Accordingly, we were able to develop an easily reproducible and reliable model allowing for repetitive morphological, dynamic and functional real-time evaluation of various parameters of muscle and skin vasculature that can be correlated with immunohistochemical and molecular analysis of the sampled flap tissue.

The surgical procedure does not require any specific surgical skills, though practice and some manual dexterity is necessary. A learning curve of about 25-30 operated animals is usually necessary to master the mounting of the dorsal skinfold chamber and flap preparation properly. In experienced hands, time for surgery averages 35 minutes. Crucial steps of flap preparation include the correct placement and outline of the flap in the center of the chamber's window with accurate positioning of the main vessels to be transected (using trans-illumination) and the meticulous removal of the gelatin-like layer above the panniculus carnosus using image-magnification to improve the image quality.

Since flap dimensions are given in millimeters, we recommend using a sliding caliper for correct flap marking. If there are any difficulties while positioning the horizontally arranged dominant vessels within the chamber's window, one should rather choose a more distal than a more proximal position of the vessels. The correct positioning of these vessels that transverse the chamber's window, guarantees transection of these while elevating the flap from distal to proximal and results in a randomly perfused flap. In other words, failure to transect these major vessels will result in an axial perfusion pattern without necrosis of the tissue under the window. The final crucial step during surgical preparation concerns the removal of the gelatin-like areolar tissue layer. Experience has shown that excessive removal damages the subjacent panniculus carnosus and so the delicate horizontally arranged muscular capillaries. Contrariwise, conservative removal results in edema-formation and eventually limited visibility of the regions of interest during microscopy. If all these steps are mastered with care, the flap very constantly develops approximately 50% necrosis 10 days after flap elevation. This allows studying various therapeutic strategies that may improve or worsen survival of the flap tissue. Finally, the method of intravital fluorescence microscopy is a well-established procedure to evaluate microvascular tissue perfusion and can be learned very quickly.

The major drawback of this model is the limited observation time of the tissue within the chamber's window of approximately 10 to 14 days following flap preparation. This is due to the progressive loosening of the skin proximal to the dorsal skinfold chamber that finally results in

sideways tilting of the chamber. Rarely, the sandwich-like, fixed skin pulls out of the chamber's frame and renders microscopy impossible. Since necrosis is most often fully demarcated between day 5 and 7 after surgery, this does not really compromise data acquisition before tilting of the chamber or pulling out of the skin within the chamber.

Advantages of the model include easy reproducibility and the potential use of genetically modified animals. The relatively small size of the window that can be assessed might however compromise the significance in translating the results into human conditions. In addition, there are anatomical differences between loose skinned animals and humans. While the animals and surgical tools have a reasonable cost-effectiveness, the hard- and software necessary to perform microscopy (epi-illumination microscope, high-resolution camera, fluorescent dyes and special software for off-line data analysis) represents a bigger investment.

Conclusion:

We present a time and cost-effective animal model in mice that allows visualization and quantification of microcirculatory parameters at high resolution. This approach represents an ideal method to analyze critically perfused musculocutaneous flap tissue and the underlying cellular mechanisms. Morphological changes of regions of interest can be repeatedly investigated and correlated with functional changes on a microvascular and cellular level. After intravital epi-fluorescence microscopy, the tissue can be further processed using histological and molecular approaches.

Disclosures

None

Acknowledgements

We thank Katharina Haberland for image editing. Funding: The senior author received a KKF Grant from the Technische Universität München to set up a new research laboratory.

References

1. McFarlane, R., De Young, G., Henry, R. The design of a pedicle flap in the rat to study necrosis and its prevention. *Plast Reconstr Surg.* **35**, 177 - 82 (1965).
2. Finseth, F., Cutting, C. An experimental neurovascular island skin flap for the study of the delay phenomenon. *Plast Reconstr Surg.* **61**, 412 - 20 (1978).
3. Petry, J. J., Wortham, K. A. The anatomy of the epigastric flap in the experimental rat. *Plast Reconstr Surg.* **74**, 410 - 3 (1984).
4. Achauer, B. M., Black, K. S., Litke, D. K. Transcutaneous PO2 in flaps: a new method of survival prediction. *Plast Reconstr Surg.* **65**, 738 - 45 (1980).
5. Vollmar, B., Menger, M. D. Assessment of microvascular oxygen supply and tissue oxygenation in hepatic ischemia/reperfusion. *Adv. Exp. Med. Biol.* **428**, 403 - 8 (1997).
6. Menger, M. D., Barker, J. H., Messmer, K. Capillary blood perfusion during postischemic reperfusion in striated muscle. *Plast Reconstr Surg.* **89**, 1104 - 14 (1992).
7. Uhl, E., Rösken, F., Curri, S. B., Menger, M. D., Messmer, K. Reduction of skin flap necrosis by transdermal application of buflomedil bound to liposomes. *Plast Reconstr Surg.* **102**, 1598 - 604 (1998).
8. Pang, C. Y., Neligan, P., Nakatsuka, T., Sasaki, G. H. Assessment of the fluorescein dye test for prediction of skin flap viability in pigs. *J Surg Res.* **41**, 173 - 81 (1986).
9. Hjortdal, V. E., Hansen, E. S., Henriksen, T. B., Kjolseth, D., Soballe, K., Djurhuus, J. C. The microcirculation of myocutaneous island flaps in pigs studied with radioactive blood volume tracers and microspheres of different sizes. *Plast Reconstr Surg.* 8 **9**, 116 - 22 (1992).
10. Pang, C. Y., Neligan, P., Nakatsuka, T. Assessment of microsphere technique for measurement of capillary blood flow in random skin flaps in pigs. *Plast Reconstr Surg.* **74**, 513 - 21 (1984).
11. Sandison, J. C. A new method for the microscopic study of living growing tissues by the introduction of a transparent chamber in the rabbit's ear. *The Anatomical Record.* **28**, 281 - 287 (1924).
12. Algire, G. H. An Adaptation of the Transparent-Chamber Technique to the Mouse. *Journal of the National Cancer Institute.* **4**: 1 – 11 (1943).
13. Lehr, H.A., Leunig, M., Menger, M.D., Nolte, D., Messmer, K. Dorsal skinfold chamber technique for intravital microscopy in nude mice. *Am J Pathol.* **4**,1055-62 (1993).
14. Barker, J. H., *et al.* An animal model to study microcirculatory changes associated with vascular delay. *Br J Plast Surg.* **52**, 133 - 42 (1999).
15. Erni, D., Sakai, H., Banic, A., Tschopp, H. M., Intaglietta, M. Quantitative assessment of microhemodynamics in ischemic skin flap tissue by intravital microscopy. *Ann Plast Surg.* **43**, 405 - 14 (1999).
16. Roesken, F., Schäfer, T., Spitzer, W. J., Vollmar, B., Menger, M. D. In vivo analysis of the microcirculation of osteomyocutaneous flaps using fluorescence microscopy. *Br J Plast Surg.* **52**, 644 - 52 (1999).
17. Harder, Y., Amon, M., Erni, D., Menger, MD. Evolution of ischemic tissue injury in a random pattern flap: a new mouse model using intravital microscopy. *J Surg Res.* **121**, 197 - 205 (2004).
18. Harder, Y., Contaldo, C., Klenk, J., Banic, A., Jakob, SM., Erni, D. Preconditioning with monophosphoryl lipid A improves survival of critically ischemic tissue. *Anesth Analg.* **100**, 1786 - 92 (2005).
19. Rezaeian, F., *et al.* Erythropoieton protects critically perfused flap tissue. *Ann Surg.* **248**, 919 – 29,doi: 10.1097/SLA.0b013e31818f678e, (2008).
20. Harder, Y., *et al.* Erythropoietin reduces necrosis in critically ischemic myocutaneous tissue by protecting nutritive perfusion in a dose-dependent manner. *Surgery.* **145**, 372 – 83, doi: 10.1016/j.surg.2008.12.001, (2009).

21. Rezaeian, F., *et al.* Erythropoietin-induced upregulation of endothelial nitric oxide synthase but not vascular endothelial growth factor prevents musculocutaneous tissue from ischemic damage. *Lab Invest.* **90**, 40 – 51, doi: 10.1038/labinvest.2009.117, (2010).
22. Rezaeian, F., Ong, MF., Harder, Y., Menger, MD. N-acetylcysteine attenuates leukocytic inflammation and microvascular perfusion failure in critically ischemic random pattern flaps. *Microvasc Res.* **82**, 28 – 34, doi: 10.1016/j.mvr.2011.03.010, (2011).
23. Rezaeian, F., *et al.* Ghrelin protects musculocutaneous tissue from ischemic necrosis by improving microvascular perfusion. *Am J Physiol Heart Circ Physiol.* **302**, 603 – 10, doi: 10.1152/ajpheart.00390.2010, (2012).
24. Rezaeian, F., *et al.* Long-term preconditioning with Erythropoietin reduces ischemia-induced skin necrosis. *Microcirculation.* doi: 10.1111/micc.12059, (2013).
25. Harder, Y., *et al.* Heat shock preconditioning reduces ischemic tissue necrosis by heat shock protein (HSP)-32-mediated improvement of the microcirculation rather than induction of ischemic tolerance. *Ann Surg.* **242**, 869 - 78 (2005).
26. Tobalem, M., *et al.* Local shockwave-induced capillary recruitment improves survival of musculocutaneous flaps. *J Surg Res.* **184**, 1196 – 204, doi: 10.1016/j.jss.2013.03.040, (2013).
27. Lindenblatt, N., Calcagni, M., Contaldo, C., Menger, MD., Giovanoli, P., Vollmar, B.A new model for studying the revascularization of skin grafts in vivo: the role of angiogenesis.*Plast Reconstr Surg.* **122**, 1669 – 80, doi: 10.1097/PRS.0b013e31818cbeb1, (2008).
28. Schweizer, R., *et al.* Morphology and hemodynamics during vascular regeneration in critically ischemic murine skin studied by intravital microscopy techniques.*Eur Surg Res.* **47**, 222 – 30, doi: 10.1159/000333088, (2011).
29. Klyscz, T., Jünger, M., Jung, F., Zeintl, H. [Cap image—a new kind of computer-assisted video image analysis system for dynamic capillary microscopy]. *Biomed. Tech.* **42**, 168 - 75 (1997).
30. Gross, J.F., Aroesty, J. Mathematical models of capillary flow: a critical review. *Biorheology.* **9**, 225 – 264 (1972).
31. Menger, M.D., Pelikan, S., Steiner, D. Microvascular ischemiareperfusion injury in striated muscle: significance of 'reflow paradox'. *Am J Physiol.* **263** (6 Part 2), H1901 – H1906 (1992).

